PRODUCTION OF HYDROGEN FROM ETHANOL USING Pt/HYDROTALCITE CATALYSTS STABILIZED WITH TUNGSTEN OXIDES.

J. L. Contreras[1], M.A. Ortiz[1], G.A. Fuentes[2], R.Luna[1], M. Gordon[1], J.Salmones[3], B. Zeifert.[3] and T. Vázquez[1].

[1]Universidad Autónoma Metropolitana-Azcapozalco CBI, Energía
Av. Sn.Pablo 180 Col.Reynosa, Azcapotzalco C.P.02200 México D.F., México.
[2] Universidad Autónoma Metropolitana-Iztapalapa CBI, IPH, México, D.F., México
[3] Instituto Politécnico Nacional, ESIQIE,Unidad Prof. ALM, México, D. F., 07738, México
[4]Instituto Mexicano del Petróleo, Eje Central Lázaro Cárdenas 152, México, D.F., México.
Tel: 53189065 ext 116, Fax 53947378, e-mail

[*] contact E-mail: jlcl@correo.azc.uam.mx

ABSTRACT

The WOx effect on Pt/hydrotalcite catalysts to produce H_2 by ethanol steam reforming was studied. The catalysts were characterized by N_2 physisorption (BET area), X-ray diffraction, Infrared (IR), Raman and UV-vis spectroscopy. The catalytic tests were made in a fixed bed reactor. The catalysts showed porous with the shape of parallel layers with a bimodal mesoporous distribution. By IR spectroscopy it was found superficial chemical groups as: -OH, H_2O, Al-OH, Mg-OH, and CO_3^{2-}. As W concentration increased, both the intensity of crystalline reflections of the catalysts and the conversion increased. Catalysts with low amount of W showed the highest H_2 selectivity and the highest stability after 7 h of reaction. The reaction products were; H_2, CO_2, CH_3CHO, CH_4 and C_2H_4. These catalysts did not produce CO and showed low selectivity to C_2H_4.

Keywords: Hydrogen, tungsten oxide, Hydrotalcite, catalysts, Platinum, ethanol

1.- INTRODUCTION

In order to produce hydrogen and its potential use in fuel cells, it has been proposed the bioethanol as a source using the catalytic steam reforming. The ethanol possesses diverse

advantages on the derived hydrocarbons of fossil sources, it is a renewable source and neutral with respect to emissions of CO_2, less toxic and it can be stored without handling risk. It can be obtained in large quantities from biomass in comparison with the methanol and gasoline.

The reaction of ethanol with steam is strongly endothermic and it only produces H_2 and CO_2 if the ethanol reacts in the most desirable way. However, other undesirable products as CO and CH_4 are also in general formed during the reaction [1]. Other reactions occur such as dehydrogenation of ethanol to CH_3CHO, dehydration to $CH_2=CH_2$, decomposition to CO and CH_4 or CO_2, CH_4 and H_2. The CH_3CHO and the $CH_2=CH_2$ are intermediary products that could be formed during the reaction at relatively low temperatures before the formation of H_2 and CO_2 and finally the formation of coke in the surface of the catalyst.

For this reaction, some authors [2-3] have demonstrated that an increase in the temperature leads to an increase in the concentration of H_2 and CO and a decrease of the CH_4 in the equilibrium [4]. They examined the thermodynamic equilibrium of this system and suggested operating at temperatures bigger than 650K, atmospheric pressure and a molar ratio of ethanol/steam of 10 in the feeding to maximize the production of H_2, minimizing the formation of CO and CH_4 and avoiding the deposition of coke on the catalyst. Other authors [1] have also carried out a thermodynamic analysis of the system. They demonstrated that an increment in the total pressure led to the decrease of H_2 and of the CO while the composition of the CH_4 in the equilibrium increases. However the system of production of H_2 and its purification has been operating at low pressure when the level of CO is reduced and the H_2 gas is rich using a metallic membrane of Pd.

Some authors carried out a thermodynamic analysis of the ethanol-water system as applied to a fuel cell and suggested that a high water-to-ethanol ratio in the feed reduced the yield of undesirable products such as CO, CH_4 and carbon [5].

The catalytic process has been studied by developing catalysts where different metals such as: Rh, Pt, Ni, Co, Zn, Fe, Cu, Au, Pd and Ru have been proven, with diverse supports of metallic oxides as Al_2O_3 [6] CeO_2 [7], MgO [8], ZnO [9], SiO_2, Sm_2O_3, TiO_2, V_2O_5 [10] La_2O_3, Y_2O_3 [11], ZrO_2 [12] among other, some alkaline promoters as K, Na and Li have been proven [13]

From many investigations, we can deduce that the activity and the distribution of products depend on the type and concentration of used metal, of the support type and the preparation method. The biggest interest is to find active catalysts that inhibit the coke formation and especially of the CO that is harmful for the fuel cells [14]. Catalysts containing Co have showed a significant enhancement of the catalytic performance in the steam reforming of ethanol [10]

The hydrotalcites are materials of wide use in catalysis because they contain a high specific area, they have the possibility of modifying their superficial characteristics and in consequence their catalytic properties, also these supports are not commonly used for the production of H_2 and they have basic sites, which are important to prevent the formation of $CH_2=CH_2$. The use of these hydrotalcites in ethanol steam reforming has been shown in other papers [15] and now in this study we combined the tungsten oxides (WOx) with the Pt-hydrotalcite catalysts in order to thermal stabilize the porous structure [16,17].

2.- EXPERIMENTAL SECTION

2.1.- Catalysts Preparation

The hydrotalcite was made by co-precipitation using two salt solutions as precursors. First, in a stirred reactor one salt solution of Mg $(NO_3)_2$ and $Al_2(NO_2)_3$ (J.T. Baker) having an atomic ratio of Mg^{2+}/Al^{3+} of 2.1. A second solution of Na_2CO_3 (5%) and NaOH (pH = 10) (Carlo Erba) was prepared. These two solutions were mixed drop by drop in water (60 drops/min) at 60°C in a simultaneous manner in a third stirred reactor, the pH of the solution was measured. The catalysts were made adding $(NH_4)_{12}W_{12}O_{41}\bullet 5H_2O$, (Aldrich) and H_2PtCl_6 in solution after the co-precipitation to get a constant amount of 0.35wt%Pt and several W concentrations: without W (sample HT), 0.5wt%W(HT05W), 0.5wt%W and Pt (HTP05W), 1wt%W and Pt (HTP1W), 2 and 3 wt% W and Pt (HTP2W and HTP3W). After this impregnation the solid suspension was stirred during 24 h at 60°C. The solid phase was washed three times with distilled water and it was dried at 120°C for 24 h and calcined at 450°C during 5 h. Finally the catalysts were reduced in H_2 at 450°C for 2 h.

2.2.- Catalysts Characterization

The solid obtained was characterized by X-ray diffraction (XRD) in a Phillips X´ Pert instrument. The XRD patterns of the samples after calcination were obtained using the CuKα radiation. Diffraction intensity was measured in the 2θ range between 5 and 70° with a 2θ step of 0.02° with 8 seconds per point, the samples were analyzed directly at room temperature. The infrared spectroscopy was made in a Perkin Elmer spectrophotometer (Spectrum-RX). An infrared beam was sent through a wafer of the sample. The wavenumber range was from 4000 to 400 cm^{-1} and the number of averaged scans was 50. N_2 physisorption a - 196°C was made in a Micromeritics 2000 instrument. Each sample was pretreated at 200°C under vacuum (1 x 10^{-4} torr). The diffuse reflectance UV-visible spectroscopic analysis (UV-vis) of the samples was made in a Varian (Cary 5E) spectrophotometer. The range of wavelength was from 3000 to 200 nm.

2.3. - Catalytic evaluation

The catalytic evaluation of ethanol steam reforming was made in a U-shaped stainless steel fixed bed reactor (7 mm internal diameter). The catalyst (1g, 100 US mesh) was charged for each of the reaction tests. The feed of the reactants comprised of a gaseous mixture of ethanol (Aldrich), water as steam and N_2 (purity 99.99%, Infra-Air Products) was supplied by a micrometric needle valve (1 ml/s). A constant mixture H_2O and CH_3CH_2OH (molar ratio of 4:1) in a N_2 stream was supplied in gas flow using two glass saturators and this mixture was vaporized and kept at 92°C before it was feed to the reaction chamber.

The temperature of the catalyst was raised at 450°C in flow of N_2 for 30 min to activate the catalyst and then the flow of reactants started at this temperature. The catalyst was held at that temperature for 30 min in order to have three analyses and for deactivation tests the catalysts were evaluated during 300 min.

The analysis of the reactants and all the reaction products was carried out online by gas chromatography. Inside an automated injection valve, the sample was divided into two portions which were then analyzed in a different way in order to obtain accurate, complete quantification of the reaction products. One of the portions was used to analyze H_2, CO, CO_2 and CH_4, using a

packet column of silica gel 12 grade 60/80 (18´x 1/8") with a thermal conductivity detector (Gow-Mac apparatus). The second portion was used to analyze CH_3CH_2OH, CH_3CHO, CH_3COCH_3, CH_2O and $CH_2=CH_2$ with a capillary column (VF-1ms, 15m x 0.25 mm) in a Varian chromatograph CP-3380 with a flame ionization detector (FID). Response factors for all products were obtained and the system was calibrated with appropriate standards before each catalytic test. The conversion (X) was calculated using the ethanol composition before and after of the reaction. The selectivity was defined as the mole fraction of each product as follows:

$$Si\ (\%) = Ni / \Sigma Nj \times 100 \qquad (1)$$

(See the nomenclature)

The water was not included.

3.- RESULTS AND DISCUSSION

3.1.- Textural properties

Both, the surface area BET and the nominal content of W are shown in Table 1. These samples were mesoporous and they showed the hysteresis of the IV type in accordance with the IUPAC classification [18-20]. At low pressures, first an N_2 adsorbate monolayer is formed on the pore surface, which is followed by the multilayer formation. The hysteresis of the isotherms could correspond with the structure of parallel plates typical of the hydrotalcites (Figure 1). It was found a W effect over the pore diameter distribution in the samples (Figure 2). Samples with 0.5wt% W (samples HT05W and HTP05W) showed a wide pore distribution (100 to 1000 Å) while the sample with 1wt%W (HTP1W) showed the most wide pore distribution (60 to 1000 Å). For the samples HTP2W and HTP3W the pore distribution was the shortest (200 to 1000 Å), (Figure 2). The addition of tungsten species to the hydrotalcite produced in this material different pore distribution. High W content (3wt%) produced average pore diameter of 500 Å and the sample with only 1wt%W produced an average pore diameter of 200 Å and wide pore

distribution. It was found that the WOx addition to the hydrotalcite decreased the pore volume and the surface area.

Table 1. Surface area and pore diameter of the Pt/WOx-Hydrotalcite catalysts. The Pt concentration remained constant (0.35wt%)

	W (% peso)	Surface Area BET (m^2/g)	Pore Volume (cm^3/g)	Pore Diameter (Å)
HT05W	0.5	257	1.1	175
HTP05W	0.5	227	1.0	187
HTP1W	1	242	1.1	187
HTP2W	2	229	0.7	122
HTP3W	3	151	0.7	191

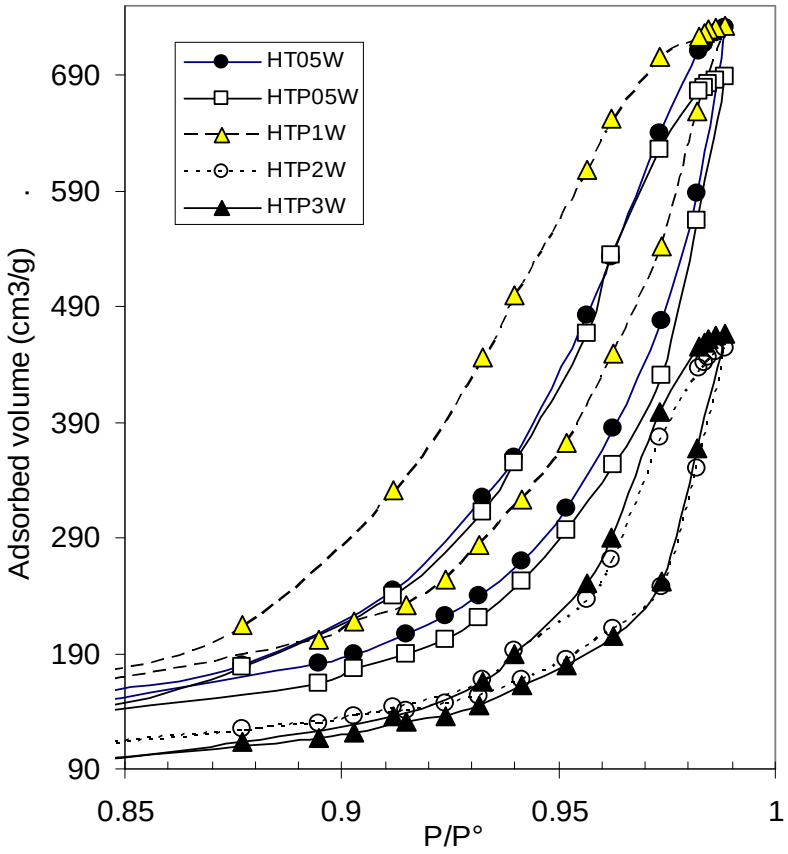

Figure 1. N_2 isotherms of the Pt /WOx-Hydrotalcite catalysts.

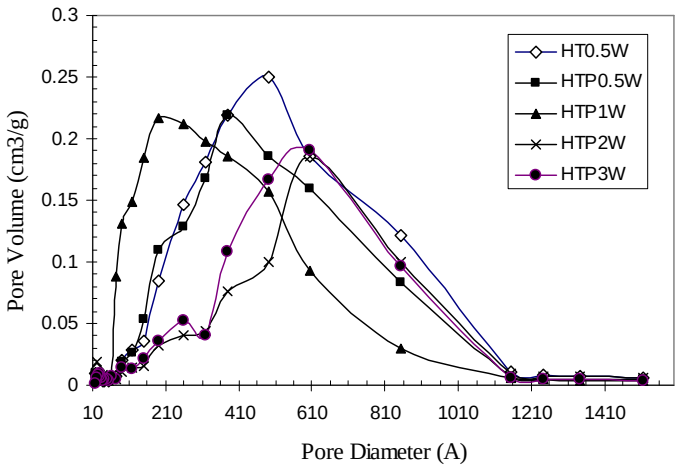

Figure 2. Pore distribution of the Pt /WOx-Hydrotalcite catalysts.

3.2.- XRD analysis

It was found symmetric intense peaks in reflections 2θ located in (003), (006), (110) and (113) (Figure 3). Additionally it was found asymmetric peaks with less intensity in (012), (015) y (018). These peaks corresponded with a laminar structure typical of hydrotalcites [15, 21]. As W concentration increased the crystalline structure of the hydrotalcite increased. The absence of other phases suggests that both W^{6+} and Al^{3+} have isomorphically replaced Mg^{2+} cations in the burcite-like layers [22]. The intensity of the diffraction lines due to the hydrotalcite phase increased by the addition of W cations, indicating that the crystallinity of the hydrotalcite phase with the W-precursor is higher than that of the Mg-Al-Hydrotalcite. An inverse behavior has observed with Ni [23].

3.3.- Infrared spectroscopy

The infrared spectrum for the sample HTP0.5W (Figure 4), showed a broad OH stretching band in the region 3400-3000 cm^{-1} and the H_2O scissoring mode band near 1600 cm^{-1} which provide evidence of the presence of water molecules. A strong band located at 1380 cm^{-1} is attributed to the presence of residual nitrate ions. Another band located at 1029 cm^{-1} is related with the

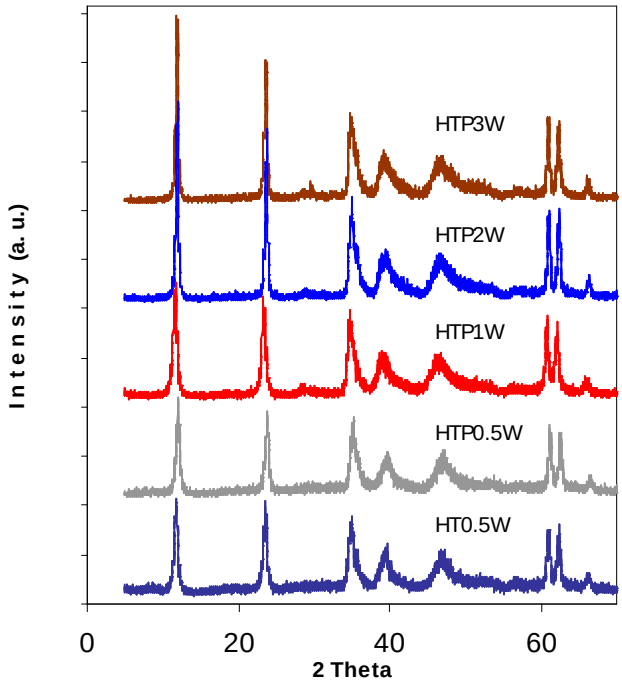

Figure 3 . X-ray diffraction of the Pt/WOx-Hydrotalcite catalysts.

symmetric C=O stretching carbonate ion which has been found in 1041cm^{-1}[24]. In the region below 1000 cm^{-1} the spectrum showed a band located in 772 cm^{-1} which is related with vibrations of –OH bending of brucite type layers [24]. The bands located at 680, 560 cm^{-1} are related with vibration modes of brucite type layers specifically the metal-oxygen symmetrical stretching. Other authors have attributed the band at 3410 cm^{-1} with hydroxil groups coordinated with Mg and Al while the vibration of the same group associated with water is a wide band between 3650-3590 cm^{-1} [25].

The antisymmetric OH stretching band located at 3460 cm^{-1} of the brucite type layers decreased as W concentration was from 0.5wt% (sample HTP0.5W) to 1 and 2 wt% (samples HTP1W and

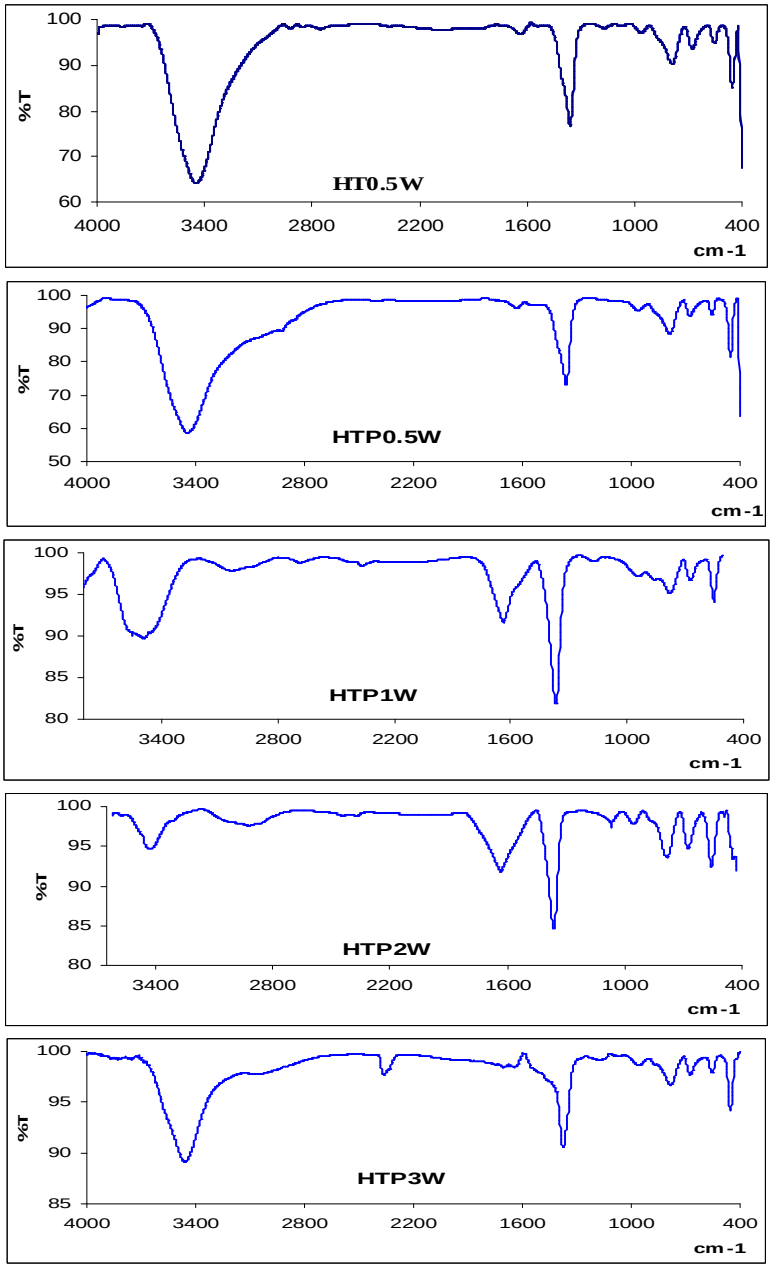

Figure 4 . Infrared spectrum of Pt/WOx-hydrotalcite

HTP2W) while the H_2O scissoring mode band at 1600 cm^{-1} increased. The analysis of the W effect on the superficial species suggested that W substituted the –OH groups of the brucite type

layers. But the intensity of this band increased again for the sample with 3wt%W so it was difficult to correlate this band with the W concentration and more experiments will be required.

3.4.- Raman spectroscopy

It was found a small band located at 490 cm^{-1} (Figure 5) which could be related with presence of O-W-O bonds on the support [26] or with the Al-O bending mode of the hydrotalcite. We did not find the band located at 950-1050 cm^{-1} related with octahedral structures of WOx which usually is found on Al_2O_3 [26]. Most of the highest frequency of Raman bands for tetrahedral and octahedral tungsten oxide compounds are considered between 740 and 1060 cm^{-1} [26], for example the highest frequency for the WO_3 is 805 cm^{-1}, for $Al_2(WO_4)_3$ is 1060 cm^{-1}, for Na_2WO_4 is 928 cm^{-1} and for $(NH_4)_{12}W_{12}O_{41}$ was 980 cm^{-1}. For $[W_{12}O_{42}]^{12-}$ supported on Al_2O_3 the major Raman bands are located at 977, 963 and 166 cm^{-1} [27] with the lowest band position attributed to the W-O-W deformation mode.

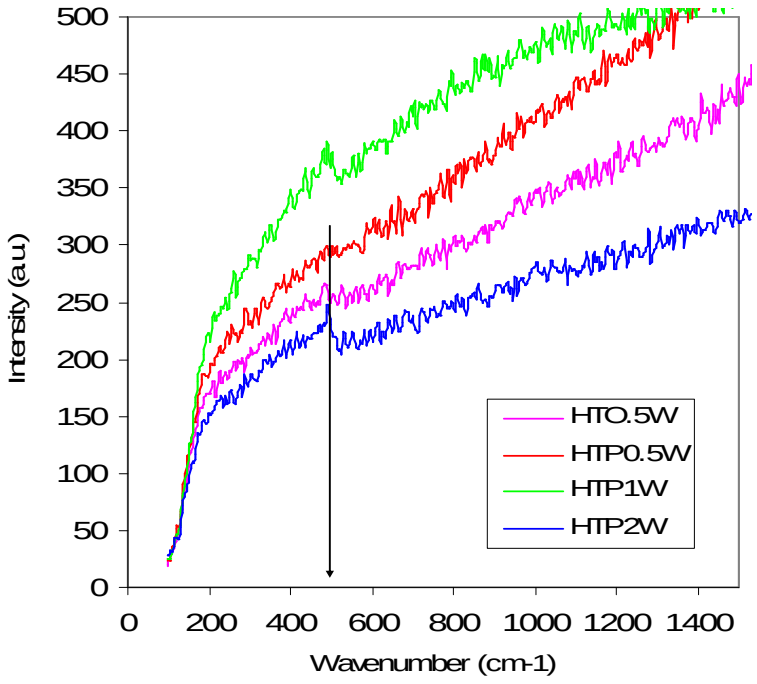

Figure 5. Raman spectroscopy of the Pt/WOx/hydrotalcites.

For W compounds, we did not find any Raman bands near 500 cm^{-1}. But the band at 500 cm^{-1} is very close to the position of the strongest band related with the Al-O- bending mode in zeolite A located at 494 and 415cm^{-1}[26]. Furthermore it is known that in crystalline alumina oxide the strongest Raman bands were found to be near 380 and 640 cm^{-1}. These spectra suggested that W^{6+} ions could be isomorphically replacing the Mg^{2+} cations in the brucite-like layers [22].

3.5.- UV-vis analysis

It was found a strong band at 230 nm for all the catalysts containing W (Figure 6). This band has been attributed to a ligand-metal charge transfer (LMCT) of the single ligand of the W=O (the W^{6+} is a cation d°) [28,29]. Usually this band increased as the W concentration increased on Al_2O_3. In these preparations the band at 230 nm increased in a similar manner suggesting that W^{6+} are present in a tetrahedral coordination [30-32]. It is known that the structure of tungstated ion in aqueous solution is highly dependent of the pH and in alkaline solutions the W^{6+} could be present as a tetrahedral monomeric ion $[WO_4]^{2-}$ [33].

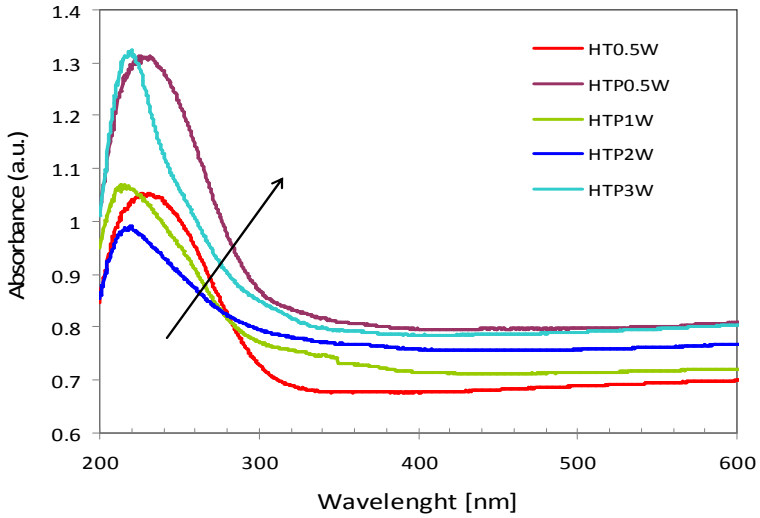

Figure 6. UV-vis of the Pt/WOx/Hydrotalcite.

3.6.- Catalytic activity

It was found a promoter effect of the W addition to the hydrotalcite prepared at 450°C (Figure 7). As W concentration increased the conversion of ethanol steam reforming increased. These catalysts produced the following products of reaction: H_2, CH_3CHO, CO_2, CH_4, $CH_2{=}CH_2$. We did not find: CH_3COOH, $CH_3CH{=}CH_2$ or other oxygenates (Figure 8).

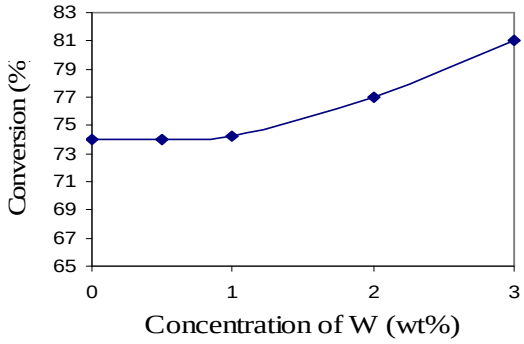

Figure 7. Effect of ethanol conversion as the W concentration increases.

The experimental results of the WOx/hydrotalcite without Pt (HT05W) showed catalytic activity of ethanol steam reforming (Figure 8). Also this type of hydrotalcite without W showed activity [15,34].

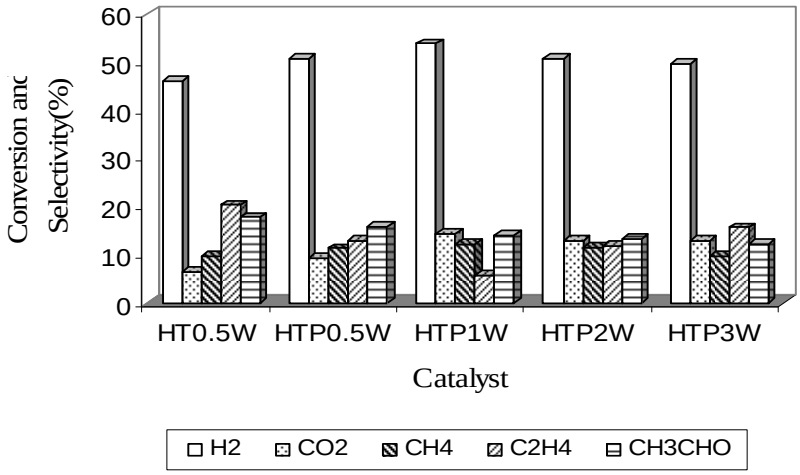

Figure 8 . Reaction products from ethanol steam reforming for the catalysts of Pt over WOx-Hydrotalcite at 450°C after 7 h of reaction.

The formation of different species on the surface has revealed that the content of oxygen of different nature such as unidentate, bidentate and formation of bicarbonate species involved surface hydroxyl groups [35]. The presence of superficial –OH on the hydrotalcite catalyzed the initial interaction of ethanol with these –OH groups to form ethoxy species which could evolve to CH_3CHO, then this compound may either evolve over the surface through alkyl elimination or form a bidentate acetate species, which suffer a C-C scission on the surface of the hydrotalcite producing CO_2, CH_4 and H_2 in the presence of water [35]. This explanation could be similar for the steam reforming of ethanol using ZnO. This oxide showed catalytic activity producing H_2, CO_2 and CH_3CHO [35]. HT05W catalyst showed a high selectivity of CH_3CHO near the 20% (Figure 8). The addition of 0.35wt%Pt in the sample HTP05W decreased the selectivity of CH_3CHO because this solid with Pt was more active.

The reaction products in Figure 8 are produced in accordance with the following reactions.

$$CH_3CH_2OH + 3H_2O \rightarrow 2CO_2 + 6H_2 \quad (1)$$

$$CH_3CH_2OH \rightarrow CH_3CHO + H_2 \quad (2)$$

$$CH_3CH_2OH + H_2O \rightarrow CO_2 + CH_4 + 2H_2 \quad (3)$$

$$CH_3CH_2OH \rightarrow CH_2{=}CH_2 + H_2O \quad (4)$$

$$CO + H_2O \rightarrow CO_2 + H_2 \quad \text{(water-gas shift reaction)} \quad (5)$$

$$CH_4 + H_2O \rightarrow CO + 3H_2 \quad (6)$$

$$CH_2{=}CH_2 + 2\,H_2O \rightarrow CH_4 + CO_2 + 2H_2 \quad (7)$$

$$CH_3CHO + H_2O \rightarrow CH_4 + CO_2 + 2H_2 \quad (8)$$

The CH_3CHO selectivity decreased as the W concentration increased and we found CH_3CHO in all the catalytic analysis, suggesting that hydrotalcite surface acted as dehydrogenation catalyst according with the reaction (2).

It can be observed that H_2 was the main product and that the ethanol steam reforming (equation 1) was the most important reaction. We did not find CO in the products because it probably reacted

with more water to produce CO_2 and more H_2 in accordance with reaction (5) (the water-gas shift reaction).

The dehydration of ethanol to $CH_2=CH_2$, reaction (4) was affected by the presence of Pt. The catalyst HT05W (free of Pt) showed the highest selectivity to $CH_2=CH_2$ (Figure 8). We did not find CO in the product distribution and the presence of Pt could convert this product into CO_2.

Ethylene and acetaldehyde are intermediate products formed from ethanol dehydration and dehydrogenation respectively, reaction (4) and reaction (2). These products promoted coke formation as other authors have reported [36]. In space times lower than 0.5 (mg of catal./ml of total flow in the inlet/min) ethylene and acetaldehyde appears between the reaction products. The yields of these products as a function of space time have a typical behavior of intermediate products [37].

The presence of W^{6+} in the hydrotalcite increased the crystalline structure by XRD (Figure 3). This physical property was proportional with the conversion, but it was not proportional with the selectivity to produce H_2 (Figure 8). From all the samples, the HTP1W catalyst showed the most wide pore distribution (Figure 2) and the highest selectivity to H_2 (55%) and CO_2. Also this catalyst showed the lowest selectivity to $CH_2=CH_2$.

The difference in H_2 selectivity between the HTP1W catalyst and the others was very small and it is difficult to assign the H_2 selectivity only at one catalyst. It is known, that the H_2 production comes from several reactions; dehydrogenation, water-gas shift conversion of CO and decomposition of oxygenated compounds. In this way, infrared studies have showed that dehydrogenation of molecularly adsorbed ethanol was proposed as a key reaction step [38]. The ethanol adsorbs molecularly to form hydrogen-bonded weakly adsorbed species and to produce strongly adsorbed molecular ethanol on the Lewis-sites of the support. It was found that high temperature treatment of the adsorbed species caused the formation of surface acetate species on the support. The presence of water lowered the temperature at which the acetate species appeared and increased the stability of monodentate ethoxide species.

The dehydrogenation of ethanol proceeded on the Pt metal producing H_2 and carbonyl-hydride surface species. At high temperature the decomposition of ethoxide (at the metal/support interface) led to the formation of H_2 [38].

3.7.- Catalytic Stability

The catalyst HTP05W (with 0.5wt%W and Pt) showed the largest stability after 7 h at 450°C (Figure 9). This behavior was very similar with the W effect in catalysts supported on Al_2O_3 [16, 17]. It was observed that catalysts with a concentration of tungsten oxide below of monolayer were stabilized and the Pt sinterization process was reduced and therefore the catalysts were active for periods of longer time. In this study the addition of W to the hydrotalcite promoted both the conversion and stability.

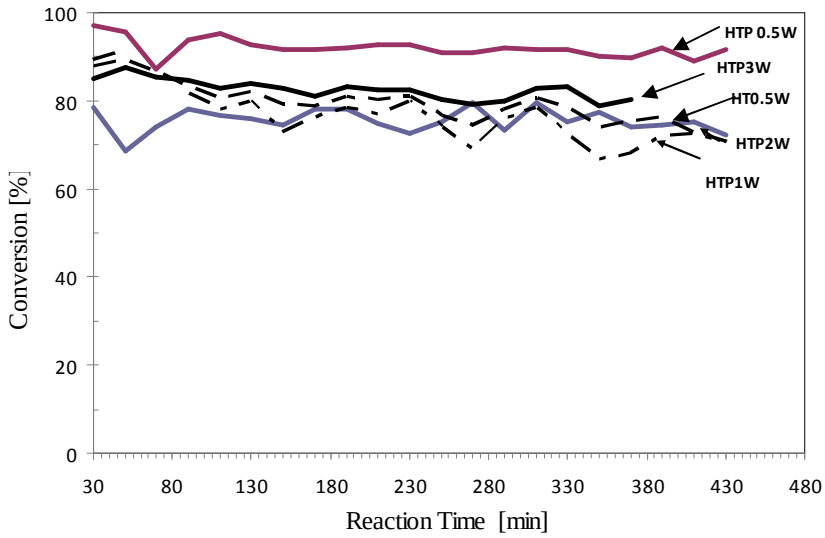

Figure 9. Catalytic deactivation of the Pt/WOx-Hydrotalcite at 450°C in the ethanol steam reforming

4.- CONCLUSIONS

It was found a promoter effect of W on the Pt/hydrotalcite catalysts. The addition of W in low amounts (0.5 and 1wt%W) produced high thermal stability and high H_2 selectivity. As W concentration increased, both the intensity of crystalline reflections of the catalysts and the conversion increased. The catalysts did not produce CO and showed low selectivity to $CH_2=CH_2$. These enhanced catalytic properties were related with a better WOx-Hydrotalcite crystallinity and the possible Pt stabilization produced by the W^{6+} ions bonded with the hydrotalcite structure. It was found superficial chemical groups as: H_2O, Al-OH, Mg-OH, and CO_3^{2-}. The Pt/hydrotalcite catalyst with the lowest W concentration (0.5wt%) showed the highest catalytic stability.

5.- ACKNOWLEDGEMENTS

The authors acknowledge the financial support of the Universidad Autónoma Metropolitana-Azcapotzalco, Iztapalapa, the Instituto Politécnico Nacional and the Instituto Mexicano del Petróleo.

6.- REFERENCES

[1] F. Aupretre, C.Descorme, D.Duprez, D.Casanave.D. Uzio, *J. Catal.* **233, 464(2005).**

[2] E.Y. García, M. A. Laborde, *Int. J. Hydrogen Energy* **16,(5), 307(1991).**

[3] K. Vasudeva, N. Mitra,P., S. Umasankar, C.Dhingra, *Int. J. Hydr.Energy* **21(1), 13(1996).**

[4] I. Fishtik,R. Alexander, R. Datta, R.,D. Geana, *Int. J. Hydrogen Energy* **25,31(2000).**

[5] S.Freni, G. Maggio, S. Cavallaro, *J. Power Sources***, 62, 67(1996).**

[6] J.P.Breen, R.Burch, , H.M. Coleman, *Appl. Catal. B: Environ* **39,65(2002).**

[7] N. Laosiripojana, S. Assabumrungrat. *Appl. Catal. B: Environ* **669,29(2006).**

[8] F. Frusteri, S. Freni, V.Spadaro, Chiodo, G. Boura, S. Donato, S. Carvallo, *Catal.Commun.* **(5) 611(2004).**

[9] N. Homs, J. Llorca, P.Ramírez de la Piscina, *Catal. Today* **116,3 (2006)361-366.**

[10] J. Llorca, N. Homs, J. Salts, P.Ramírez de la Piscina, *J. of Catal.* **209, 306(2002).**

[11] J. Sun, P. Xin- W Q. Feng., *Int. J. Hydrogen Energy* **30, 437(2005).**

[12] C.Diagne, H.Idriss, K.Pearson, M.A.Gómez-García *Comptes l'Académie Rendus gives Sciences* **7, 617-622(2004)**

[13] C. L. Hernández and V. Kafarov. *Proceedings of Simposio Iberoamericano de Catálisis Anais do XXSICAT, FISOCAT, Gramado Brazil* **17-22 Sept. p1-8(2006).**

[14] V Mas, M. L.Dieuzeide, R.Tejeda, M. Jobbagy, G. Baronetti, N. Amadeo, M. Laborde, *Proceedings of Simposio Iberoamericano de Catálisis. Anais do XX SICAT –FISOCAT, Gramado, Brazil, Sept.* **17-22(2006)**

[15] J.L.Contreras, J.Salmones, L.A. García, A. Ponce, B. Zeifert and G.A. Fuentes, *J. of New Materials for Electrochemical Systems* **11,109-117, (2008).**

[16] J.L.Contreras, G.A.Fuentes, J.Salmones, B. Zeifert *J. of Alloys and Compounds 483,* **371-373(2009).**

[17] J. L. Contreras, G.A. Fuentes. J. Salmones, B. Zeifert. *Mater. Res. Soc. Symp. Proc. Vol. 1279, Materials Research Society,* **(2010) 123-141.**

[18] K. Sing, D. Everett, R. Haul, L. Moscou, R. Pierotti, J. Rouquerol, and T. Siemieniewska, *Pure Appl. Chem.* **57, 603 (1985).**

[19] L. D. Gelb, K. E. Gubbins, R. Radhakrishnan, and M. Sliwinska-Bartkowiak, *Reports on Progress in Physics* **62, 1573 (1999).**

[20] S. Lowell, J. E. Shields, M. A. Thomas, and M. Thommes, *Characterization of Porous Solid and Powders: Surface Area, Pore Size and Density,Kluwer Academic Publischers***, 2004**

[21] I.O.Cruz, N.F.P.Ribeiro, D.A.G. Aranda, M.M.V.M. Souza, *Catalysis Comm.* **92606-,2611(2008).**

[22] A.C.C. Rodríguez,C.A. Enríquez, J.L.F. Monteiro, *Mater. Res.* **6,563(2003).**

[23] T. Shishido, M. Sukenobu, H. Morioka, R. Furukawa, H. Shirahase, K. Takehira, *Catal. Lett.***73, 21(2001).**

[24] C.Resini, T. Montenari, L. Barattini, G. Ramis, G. Busca, S. Presto, P. Riani, R. Marazza, M. Sisani, F. Marmottini, U. Costantino, *Appl. Catal.A: General,* **355,83-93(2009).**

[25] María de los Ángeles Ocaña Zarceño, *Síntesis de Hidrotalcitas y Materiales Derivados: Aplicaciones en Catálisis Básica. Tesis de Doctorado, Universidad Complutense de Madrid* **(2005).**

[26] J.M. Stencel, *"Raman Spectroscopy for Catalysis", Van Nostrand Reinhold, New York* **82-85(1990).**

[27] Busey, R.H. and O.L. Keller Jr., *J. Chem. Phys.* **41,215(1964).**

[28] A. Bartecki and Dembicka, D. *J. of Inorg. and Nuclear Chem.***V.29,I.12,2907-2916(1967).**

[29] J.L.Contreras and G.A.Fuentes, *Studies in Surface Science and Catalysis,***Vol. 101 Edit.** *B.Delmon and J.T. Yates, Elsevier* **1195-1204(1996).**

[30] A. Iannibello, L.Villa and S. Marengo, *Gazzetta Chimica Italiana***,109, 521(1979).**

[31] L. Salvati, L.E.Makovsky, J.M. Stencel, F. R. Brown, D.M. Hercules,*J. Phys.Chem.***85,3700-3707(1981).**

[32] J.A. Horsley, I.E. Wach, J.M. Brown, G.H. Via, F.D.Hardcastle,*J.Phys. Chem***.91(15) (1987)4014-4020.**

[33] W.P. Griffith and T.D. Wickins, *J.Chem.Soc. A.* **1087(1966).**

[34] J. Salmones, B. Zeifert, M.H. Garduño, J. Contreras L., D. R. Acosta, A. Romero S. and L.A. García, *Catal. Today* **133-135, 886-890 (2008)**

[35]- J.Llorca, N. Homs, P.Ramírez de la Piscina, *J. of Catal.* **227, 556-560(2004).**

[36] J.R. Rostrup-Nielsen, N. Hojlund in: *J. Oudar, H. Wise (Eds.), Deactivation and Poisoning of Catalyst, Marcel Dekker, New York, Basel***, p.57(1985).**

[37] J. Comas, F. Mariño, M.Laborde, N. Amadeo. *Chem Eng. J.* **98, 61-68(2004).**

[38] A. Erdohelyi, J. Rasko, T. Kecskes, M. Toth, M.DömÖk, K.Baán, *Catal. Today* **V.116,3, 15 Aug (2006)367-376.**